Received 10 April 2012
Revised 2 September 2012
Accepted 21 January 2013

Active flow control of airfoil using mesh/meshless methods coupled to hierarchical genetic algorithms for drag reduction design

Hong Wang and Jyri Leskinen
Department of Mathematical Information Technology, University of Jyväskylä, Jyväskylä, Finland
Dong-Seop Lee
International Center for Numerical Methods in Engineering, Barcelona, Spain, and
Jacques Périaux
Department of Mathematical Information Technology, University of Jyväskylä, Jyväskylä, Finland and International Center for Numerical Methods in Engineering, Barcelona, Spain

Abstract

Purpose – The purpose of this paper is to investigate an active flow control technique called Shock Control Bump (SCB) for drag reduction using evolutionary algorithms.

Design/methodology/approach – A hierarchical genetic algorithm (HGA) consisting of multi-fidelity models in three hierarchical topological layers is explored to speed up the design optimization process. The top layer consists of a single sub-population operating on a precise model. On the middle layer, two sub-populations operate on a model of intermediate accuracy. The bottom layer, consisting of four sub-populations (two for each middle layer populations), operates on a coarse model. It is well-known that genetic algorithms (GAs) are different from deterministic optimization tools in mimicking biological evolution based on Darwinian principle. In HGAs process, each population is handled by GA and the best genetic information obtained in the second or third layer migrates to the first or second layer for refinement.

Findings – The method was validated on a real life optimization problem consisting of two-dimensional SCB design optimization installed on a natural laminar flow airfoil (RAE5243). Numerical results show that HGA is more efficient and achieves more drag reduction compared to a single population based GA.

Originality/value – Although the idea of HGA approach is not new, the novelty of this paper is to combine it with mesh/meshless methods and multi-fidelity flow analyzers. To take the full benefit of using hierarchical topology, the following conditions are implemented: the first layer uses a precise meshless Euler solver with fine cloud of points, the second layer uses a hybrid mesh/meshless Euler solver with intermediate mesh/clouds of points, the third layer uses a less fine mesh with Euler solver to explore efficiently the search space with large mutation span.

Keywords Hierarchical genetic algorithms, Mesh/meshless method, Inverse problems, Shock Control Bump, Drag reduction, Flow, Aerodynamics

Paper type Research paper

Engineering Computations: International Journal for Computer-Aided Engineering and Software
Vol. 30 No. 4, 2013
pp. 562-580

0264-4401
DOI 10.1108/02644401311329370

1. Introduction

The drag reduction of transonic civil aircraft is one of the most important tasks in aerodynamics design. Despite continuous efforts in aerodynamic shape design over last two decades, the drag reduction at a given flight condition remains a critical challenge to aircraft designers (Qin *et al.*, 2004, 2008; Lee *et al.*, 2010). To improve drag reduction substantially, it is crucial to use a methodology that couples an efficient optimization method with an accurate computational fluid dynamic (CFD) analyzer.

In this paper, a methodology that combines hierarchical genetic algorithms (HGAs) (Sefrioui and Périaux, 2000; Pettey *et al.*, 1987; Gorges-Schleuter, 1992; Schlierkamp-Voosen and Muhlenbein, 1994) and mesh/meshless methods (Batina, 1992; Belytschko *et al.*, 1994; Ghosh and Deshpande, 1995; Morinishi, 2001; Chen and Shu, 2005; Chen, 2003; Luo and Baumy, 2005; Ma *et al.*, 2006) to improve the optimization efficiency in terms of solution accuracy and computational cost is developed. This study investigates among several active flow control techniques one device called shock control bump (SCB) (Qin *et al.*, 2004, 2008; Lee *et al.*, 2010) which was introduced earlier to generate a pre-shock isentropic compression wave in order to reduce the total drag over the airfoil at transonic speeds.

Iterative CFD methods for solving the Euler equations using traditional mesh methods have been pioneered by Godunov (1969) in the late 1960s and popularized by many CFD investigators like (Van Leer, 1979; Roe, 1981; Osher, 1983; Jameson *et al.*, 1981, 1986; Pulliam and Steger, 1985, 1986; Berger and LeVeque, 1989) and many others who pointed out successively numerous theoretical and numerical inherent advantages. Concurrently, meshless methods which allow more flexibility for computing flows around complex configurations by replacing the mesh topology constraint by clouds of points have been actively pursued in different application fields since the late 1970s (Batina, 1992; Belytschko *et al.*, 1994; Ghosh and Deshpande, 1995; Morinishi, 2001; Chen and Shu, 2005, 2003; Luo and Baumy, 2005). More recently, a hybrid mesh/meshless algorithm has been introduced. The method uses a weighted least squares (WLS) fitting of the conserved flux variables using clouds of points in the vicinity of the body and a finite volume method (FVM) in the rest of the computational domain (Ma *et al.*, 2006).

Over the past two decades, evolutionary algorithms (EAs) have become one of the most widely used optimization methods. Many researchers have proposed innovative approaches (cf. Goldberg, 1989; Deb, 2002; Michalewicz, 1992; Miettinen, 1999, among many others). The HGA (Sefrioui and Périaux, 2000; Pettey *et al.*, 1987; Gorges-Schleuter, 1992; Schlierkamp-Voosen and Muhlenbein, 1994) studied in this paper use three hierarchical topological. The top layer has a single population with two child populations in the intermediate layer, which in turn have two child populations on the bottom layer resulting in a total of seven populations. The HGAs allow the use of multi-fidelity flow analyzers as follows: high fidelity models on the top layer; intermediate fidelity models on the intermediate layer and low fidelity models on the bottom layer. In the HGA optimization procedure, each population is handled by a GA and the best genetic information obtained in the lower layers migrates to the closest upper layer for refinement, respectively.

In order to take a full benefit of hierarchical topology, each layer uses a different flow model and a different level of discretization. The following mathematical models are implemented: the top layer uses a precise meshless or mesh Euler solver with fine cloud of points or mesh elements, respectively. The middle layer uses a hybrid mesh/meshless

Euler solver with intermediate mesh elements/clouds of points. The bottom layer uses a mesh Euler solver with a coarse mesh in order to explore efficiently the search space with a large mutation span.

Two applications are considered in this paper. First, a CFD position reconstruction problem for a single NACA0012 airfoil is studied. The second test case concerns the shape optimization of a single RAE5243 airfoil at fixed lift with a Bézier spline parameterized SCB. Numerical results illustrate how the optimal shape of the SCB can modify and control the flow features over an airfoil at transonic speeds and how the total drag is reduced compared to the drag value of the baseline design. The above methodology demonstrates also how HGAs can improve the efficiency of the optimization in the terms of computational cost and design quality.

The content of the paper is organized as follows. Section 2 introduces the fast artificial dissipation (AD) adjusted meshless method for solving the nonlinear PDEs Euler equations and a dynamic cloud strategy based on Delaunay graph mapping used to move points during the optimization procedure. In Section 3, the HGA-based evolutionary optimization using mesh and meshless Euler models with different discretization levels is described in detail and is validated using a simple position reconstruction problem. Section 4 presents the results of a practical CFD application, reduction of wave drag around an airfoil by optimizing the shape of an SCB. Finally, Section 5 concludes overall numerical results and suggests future lines of research extending the present paper to more complex models and applications.

2. Methodology: a meshless Euler analyzer

2.1 Governing equations

The Euler equations represent the conservation principle for mass, momentum and energy of inviscid fluids. In a two-dimensional Cartesian coordinate system, the Euler equations are expressed in the following form:

$$\frac{\partial \mathbf{W}}{\partial t}+\frac{\partial \mathbf{E}}{\partial x}+\frac{\partial \mathbf{F}}{\partial y}=0 \tag{1}$$

where t is the time, (x, y) are the Cartesian coordinates. The vectors of conservative variables $\mathbf{W}$, convective fluxes $\mathbf{E}$ and $\mathbf{F}$ have the following components:

$$\mathbf{W}=\begin{bmatrix}\rho\\ \rho u\\ \rho v\\ e\end{bmatrix}\quad \mathbf{E}=\begin{bmatrix}\rho u\\ \rho u^2+p\\ \rho uv\\ (e+p)u\end{bmatrix}\quad \mathbf{F}=\begin{bmatrix}\rho v\\ \rho uv\\ \rho v^2+p\\ (e+p)v\end{bmatrix} \tag{2}$$

where ρ is the density, u is the x-velocity component, v is the y-velocity component, p is the pressure, and e is the total energy per unit volume. For an ideal gas, e can be written as:

$$e=\frac{p}{\gamma-1}+\frac{1}{2}\rho(u^2+v^2) \tag{3}$$

where γ is the ratio of specific heat. Additionally, the equation of state is given by:

$$p = \rho \bar{R} T$$

where T is the static temperature and $\bar{R}$ is the ideal gas constant.

2.2 Spatial discretization

The WLS method (Chen and Shu, 2005) is used to approximate the spatial first order derivatives, and in cloud $C(i)$, equation (1) becomes:

$$\left.\frac{\partial \mathbf{W}}{\partial t}\right|_i + \left(\frac{\partial \mathbf{E}}{\partial x} + \frac{\partial \mathbf{F}}{\partial y}\right)_i = 0 \tag{4}$$

For the convective fluxes, let:

$$\mathbf{Q}_i = \left(\frac{\partial \mathbf{E}}{\partial x} + \frac{\partial \mathbf{F}}{\partial y}\right)_i \tag{5}$$

According to the WLS method, the above formula can be written as:

$$\mathbf{Q}_i = \sum \alpha_{ik}\mathbf{E}_{ik} + \sum \beta_{ik}\mathbf{F}_{ik} \tag{6}$$

where α_{ik} and β_{ik} are the coefficients obtained by the WLS method. Adding equations (6) to (1), the approximated governing equation can be written as follows:

$$\frac{d\,\mathbf{W}_i}{dt} = -(\mathbf{Q}_i - \mathbf{D}_i) \tag{7}$$

where (Blazek, 2001):

$$\mathbf{D}_i = \sum_{k=1}^{N} d_{ik} \tag{8}$$

$$\begin{aligned}
d_{ik} &= \varepsilon_{ik}^{(2)}(\mathbf{W}_k - \mathbf{W}_i) - \varepsilon_{ik}^{(4)}(\nabla^2\mathbf{W}_k - \nabla^2\mathbf{W}_i)\\
\varepsilon_{ik}^{(2)} &= K^{(2)}\lambda_{ik}\max(\nu_i, \nu_k)\\
\varepsilon_{ik}^{(4)} &= \lambda_{ik}\max\left[0, K^{(4)} - \varepsilon_{ik}^{(2)}\right]\\
\nu_i &= \frac{|\nabla^2 P_i|}{\sum_{k=1}^{N}(P_i + P_k)}\\
\nabla^2\mathbf{W}_i &= \sum_{k=1}^{N}\mathbf{W}_k - N\mathbf{W}_i
\end{aligned} \tag{9}$$

$$\lambda_{ik} = |\alpha_{ik}u + \beta_{ik}v| + c\sqrt{\alpha_{ik}^2 + \beta_{ik}^2} \tag{10}$$

where $c = \sqrt{\gamma p/\rho}$ is the local speed of sound and N is the total number of could of points in node i.

2.3 Temporal discretization

In cloud $C(i)$, the semi-discretized Euler equations are written as follows:

$$\left.\frac{\partial \mathbf{W}}{\partial t}\right|_i = \mathbf{R}_i \tag{11}$$

where $\mathbf{R}_i$ is the residual value. An explicit scheme is used for time discretization on the above equation yielding:

$$\frac{\mathbf{W}_i^{n+1} - \mathbf{W}_i^n}{\Delta t} = \mathbf{R}_i \tag{12}$$

The superscripts n and $(n+1)$ denote the time levels. Here $\mathbf{W}^n$ refers to the flow solution at the present time t, and $\mathbf{W}^{n+1}$represents the solution at the time $(t+\Delta t)$. An explicit five-stage Runge-Kutta time integration scheme is used:

$$\begin{cases} \mathbf{W}_i^{(0)} = \mathbf{W}_i^n \\ \mathbf{W}_i^{(1)} = \mathbf{W}_i^{(0)} + \alpha_1 \Delta t_i \mathbf{R}_i^{(0)} \\ \mathbf{W}_i^{(2)} = \mathbf{W}_i^{(0)} + \alpha_2 \Delta t_i \mathbf{R}_i^{(1)} \\ \mathbf{W}_i^{(3)} = \mathbf{W}_i^{(0)} + \alpha_3 \Delta t_i \mathbf{R}_i^{(2)} \\ \mathbf{W}_i^{(4)} = \mathbf{W}_i^{(0)} + \alpha_4 \Delta t_i \mathbf{R}_i^{(3)} \\ \mathbf{W}_i^{(5)} = \mathbf{W}_i^{(0)} + \alpha_5 \Delta t_i \mathbf{R}_i^{(4)} \\ \mathbf{W}_i^{n+1} = \mathbf{W}_i^{(5)} \end{cases} \tag{13}$$

where $\alpha_k (k = 1, 2, 3, 4, 5)$ represents the stage coefficients:

$$\alpha_1 = \frac{1}{4}, \quad \alpha_2 = \frac{1}{6}, \quad \alpha_3 = \frac{3}{8}, \quad \alpha_4 = \frac{1}{2}, \quad \alpha_5 = 1$$

The major disadvantage of the explicit scheme is that the time step Δt_i is restricted by the Courant-Friedrichs-Lewy (CFL) stability condition.

2.4 Acceleration techniques

In order to accelerate the convergence, a local time stepping method and an implicit residual averaging method are employed in this study.

The local time step Δt_i of discrete point is given by the following equation (Blazek, 2001):

$$\Delta t_i = \frac{C_{CFL}}{\sum_{k=1}^{N} |\alpha_{ik} u + \beta_{ik} v| + c\sqrt{\alpha_{ik}^2 + \beta_{ik}^2}} \tag{14}$$

where C_{CFL} denotes the coefficient of CFL.

In the time marching equation, let $\mathbf{R}_i$ represent the residual at node i. In the meshless method, a new residual can be given by (Blazek 2001):

$$\mathbf{R}_i' = \frac{\mathbf{R}_i + \varepsilon \sum_{k=1}^{N} \mathbf{R}_k'}{1 + \varepsilon N} \quad (15)$$

where $\varepsilon = [0.2, 0.5]$. It can be accomplished by performing two Jacobi iterations. The parameter N refers to the total number of cloud of points in node i. The above technique allows the CFL number to be increased to two or three times when compared to the unsmoothed value. In the present study, the CFL number is increased from $2\sqrt{2}$ to 5.

2.5 Dynamic cloud method based on Delaunay graph mapping strategy

In order to simulate the relative movement of boundary geometries in inverse and shape optimization problems, it is required that the cloud of points has the ability to move with the rigid body boundaries. Hence, a fast and efficient dynamic cloud method based on the Delaunay graph mapping strategy (Liu *et al.*, 2006) is adopted here.

As shown in Figure 1, a Delaunay triangulation of the computational field is set up by using the given points located on the boundaries for a NACA0012 airfoil. Then, the triangulation is contained for every point $P(x, y)$ in the computational field. If the points of every element are notated as $E_1(x_1, y_1)$, $E_2(x_2, y_2)$, $E_3(x_3, y_3)$, the coordinates of point P can be expressed as:

$$\begin{cases} x = a_1x_1 + a_2x_2 + a_3x_3 \\ y = a_1y_1 + a_2y_2 + a_3y_3 \end{cases} \quad (16)$$

where $a_1 = S_1/S$, $a_2 = S_2/S$, $a_3 = S_3/S$, S, S_1, S_2, S_3 are the relevant triangle's areas (Liu *et al.*, 2006). Then, all the background points are adjusted based on the movement of the boundary points. Coordinates of the relevant triangle become $E_1(x'_1, y'_1)$, $E_2(x'_2, y'_2)$ and $E_3(x'_3, y'_3)$, and the new coordinates of point P can be denoted as:

$$\begin{cases} x' = a_1x'_1 + a_2x'_2 + a_3x'_3 \\ y' = a_1y'_1 + a_2y'_2 + a_3y'_3 \end{cases} \quad (17)$$

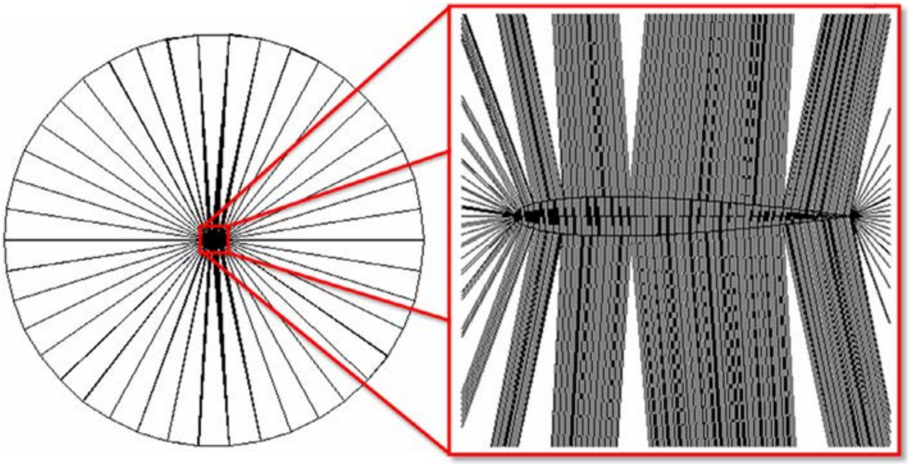

Figure 1.
Global and close-up views of a Delaunay graph in the case of a NACA0012 airfoil

Figure 2 shows the moved cloud of points for a 30° airfoil pitch using a spring analogy method described in Farhat *et al.* (1998) while Figure 3 shows the same using the Delaunay graph mapping strategy. It is apparent that a better result can be achieved using the Delaunay graph mapping strategy in order to ensure the flow field points following the movements of the body boundaries without any iterations (Wang *et al.*, 2010).

2.6 Validation of the fast AD adjusted meshless method

For validating the AD adjusted meshless method, a single RAE5243 airfoil in the flow conditions at Mach number 0.75 and fixed lift coefficient as 0.45819 is tested using the fast AD adjusted meshless method and the FVM described in Jameson *et al.* (1981).

Figure 4 shows both a global view and a close-up view of the cloud of points distributed around a single RAE5243 airfoil. Figure 5 shows both the global view and the close-up of the mesh distributed around the same airfoil. For the meshless method, a total of 6,013 nodes were used in the global domain, whereas 11,576 mesh elements were used for the mesh method. Figure 6 shows the comparison of surface pressure coefficients for this test case using the fast AD adjusted meshless method and the FVM.

In order to satisfy the fixed lift coefficient constraint at 0.45819, several iterations based on the angle of attack have been done for both the fast AD adjusted meshless method and the FVM. Figure 7 shows the comparison of convergence history for the last iteration using the meshless method and the standard mesh method. As shown in the histogram in Figure 8, the meshless method for the last iteration saves 71 percent iteration cost compared to the FVM. In terms of the CPU time cost in total, for the meshless method saves 52 percent of the cost compared to the FVM.

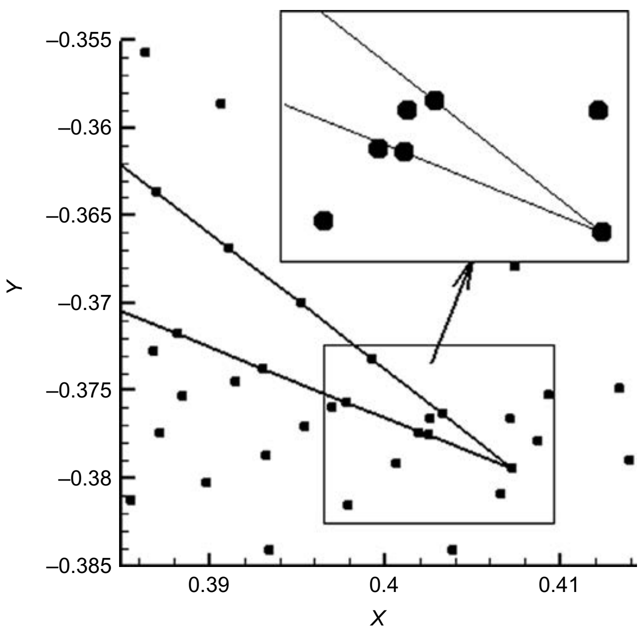

Figure 2.
Moved cloud of points for a 30° airfoil pitch using the spring analogy method

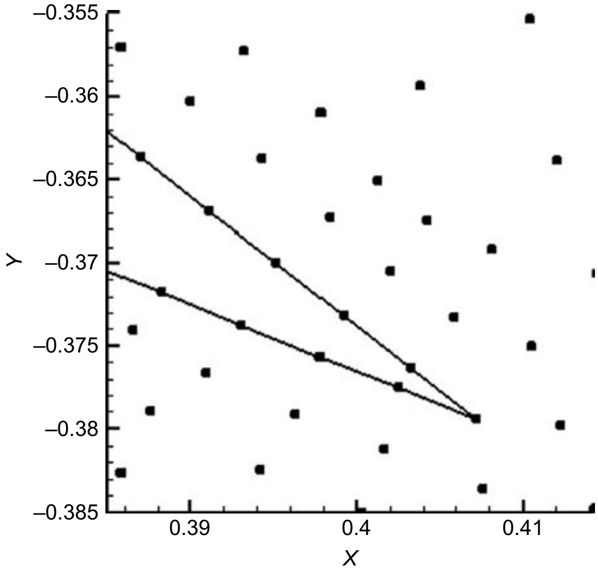

Figure 3.
Moved cloud of points for a 30° pitching airfoil using the Delaunay graph mapping strategy

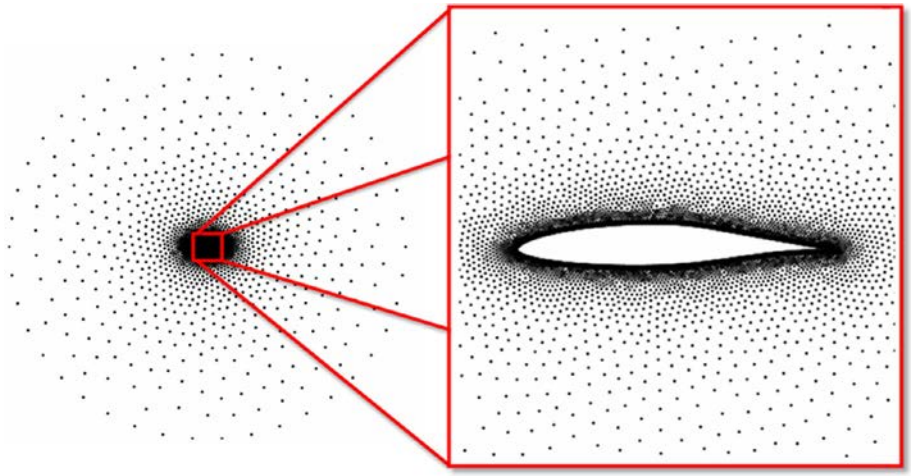

Figure 4.
Global and close-up views of the cloud of points for the RAE5243 airfoil

3. Methodology: a HGA optimizer

3.1 HGA with multiple models

Modern design problems need suitable and efficient optimizers in order to find acceptable solutions. In many realistic optimization problems, this requires the use of global optimization algorithms. Among the most successful and widely used stochastic approaches are the EAs (Sefrioui and Périaux, 2000; Pettey *et al.*, 1987; Gorges-Schleuter, 1992; Schlierkamp-Voosen and Muhlenbein, 1994; Goldberg, 1989; Deb, 2002; Michalewicz, 1992; Miettinen, 1999) which are based on the Darwinian principle of evolution by

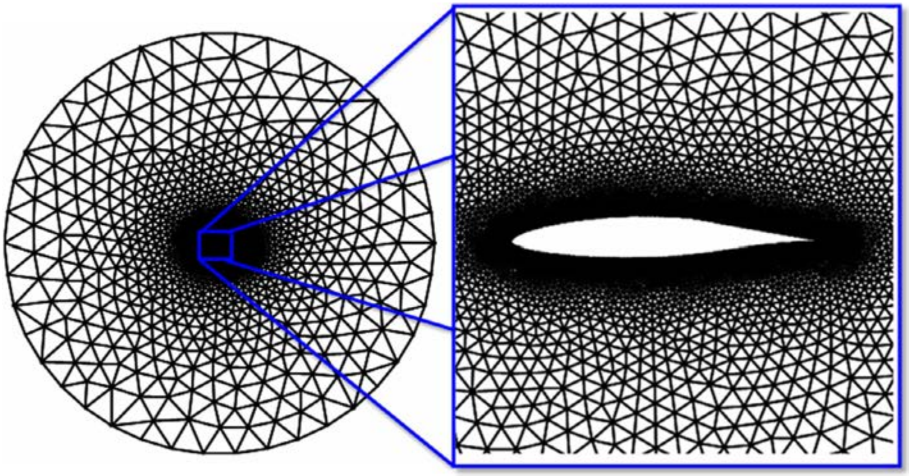

Figure 5.
Global and close-up views of the unstructured mesh around the RAE5243 airfoil

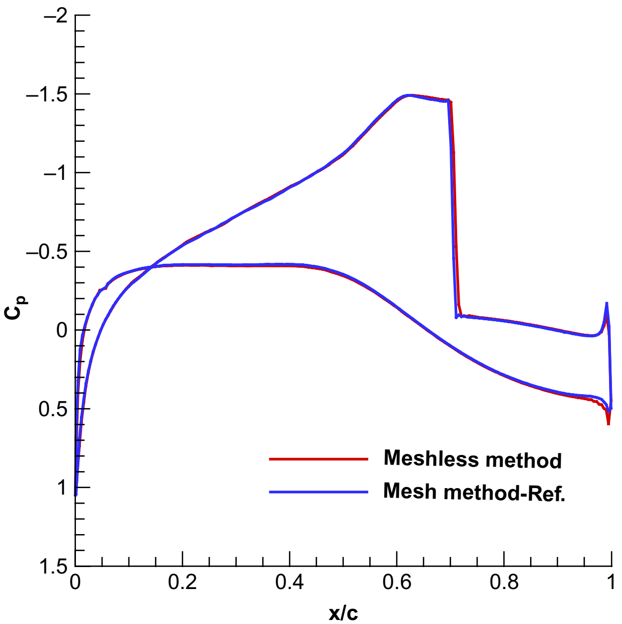

Figure 6.
Comparison of surface pressure coefficient on the RAE5243 airfoil

natural selection. The EAs do not use information on the function gradients which makes them ideal for multimodal and nonsmooth optimization. Furthermore, they can be easily implemented as "black box" which makes their implementation straightforward.

The HGAs (Sefrioui and Périaux, 2000; Pettey *et al.*, 1987; Gorges-Schleuter, 1992; Schlierkamp-Voosen and Muhlenbein, 1994) are a special class of the island-model GAs. They use a hierarchical topology (the topology used in this paper is shown in Figure 9).

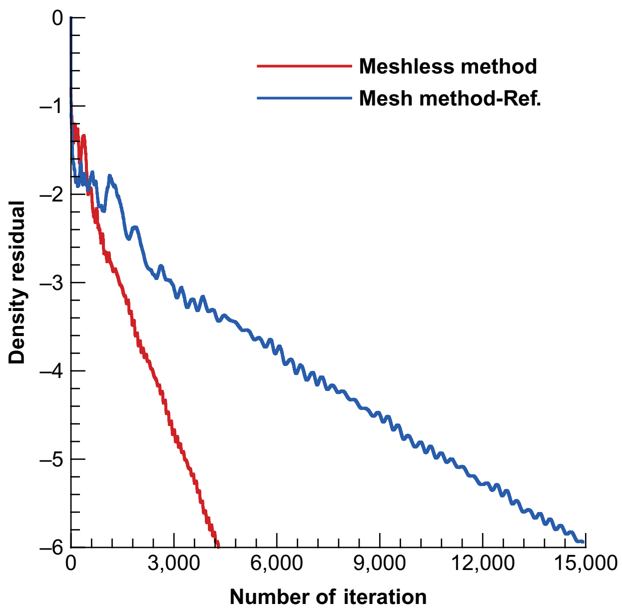

Figure 7.
Comparisons of convergence history for the RAE5243 airfoil

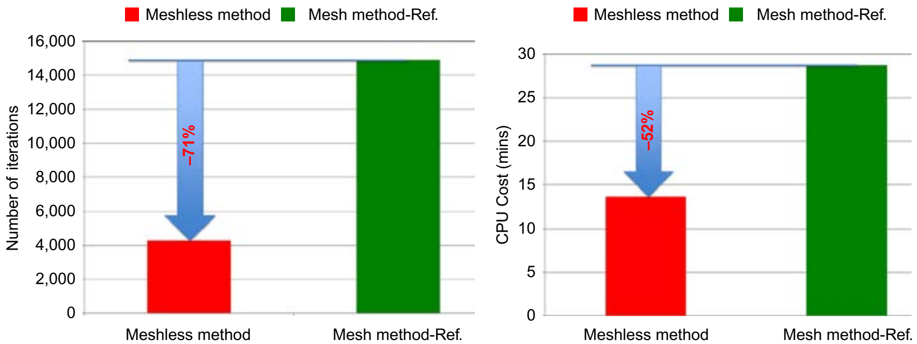

Figure 8.
Comparisons of convergence history in terms of number of iterations (left) and CPU cost (right) in minutes for the RAE5243 airfoil

Unlike the standard multi-population GAs, they operate on different models of varying accuracy. In addition, the genetic operators can vary between the different layers. On the coarse bottom layer, the objective function evaluation can be cheaper allowing an explorative algorithm; on the accurate top level, the algorithm can exploit the high-quality solutions.

In this paper, three hierarchical layers with seven populations are used. As shown in Figure 9, each node runs an individual GA with own specific input parameters. The top layer consists of a single population with an exploitative GA, the middle layer consists of two populations with intermediate GAs and the bottom layer consists of four populations with highly explorative GAs. The interaction between the populations is limited, only selected individuals are passed between the populations allowing a easy

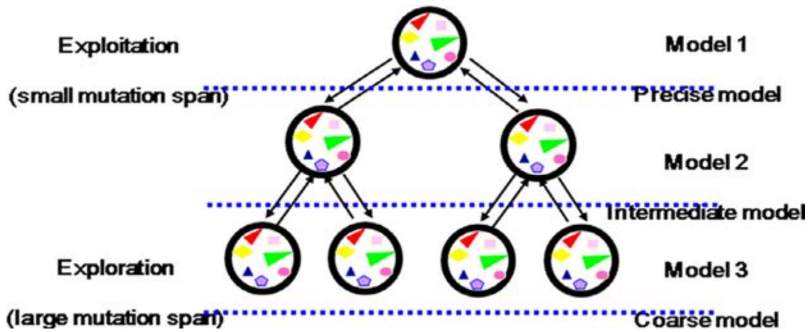

Figure 9.
Hierarchical topology

implementation in a parallelized environment. In addition, the hierarchical approach allows the use of multi-fidelity flow analyzers as follows: high fidelity (precise) models on the top layer; intermediate fidelity models on the middle layer and low fidelity (coarse) models on the bottom layer.

The HGAs also differ from island-model GAs in the way how individuals migrate between the populations. In this paper, the elite individuals from the lower populations migrate upwards replacing the worst individuals. In order to maintain diversity, the migration downwards is done using random individuals. After migrating, the individuals are reevaluated in order to make their fitness values comparable to the other individuals in the same layer.

3.2 Validation of the hierarchical approach: reconstruction of the position of a single NACA0012 airfoil

In order to validate the hierarchical approach, it is implemented numerically on a simple model reconstruction problem. Let one airfoil oscillate in pitch about its quarter chord. The rotating angle α is the single design parameter. The objective function is the minimization of the square error of the target and prescribed surface pressure coefficient vectors C_p and C_p^*:

$$\min f(\alpha) = \sum_{i=1}^{M} \left| C_p(\alpha) - C_p^*(\alpha^*) \right|_i^2 \tag{18}$$

where M is the total number of points distributed on the surface of the airfoil. The allowed range is search space is $\alpha \in [-5.0°, 5.0°]$; $\alpha^* = 0°$ denotes the prescribed angle position of the airfoil.

A HGA optimizer with multiple fidelity models is tested on the position reconstruction problem and compared to the standard GA approach. For genetic operators, the blending crossover (Eshelman and Schaffer, 1993) and Gaussian mutation on real-valued chromosomes are used. Tournament selection is used with the tournament value of 0.75 for selecting the parents. The number of offspring produced in each generation is twice the size of the parent populations. The best offspring and elites from the previous generation are selected for the next generation. Three elite individuals are selected for upwards migration, and three random individuals for downwards migration. The algorithms are terminated after 50 generations. The algorithm parameter values are listed on Table I.

For the high-fidelity model (Model 1), the fast AD adjusted meshless method and the FVM approach are applied. The intermediate model (Model 2) uses hybrid mesh/meshless method. Finally, the low-fidelity model (Model 3) uses the FVM. The models use 290, 135, and 68 nodes on the NACA0012 airfoil, respectively.

Figure 10 shows convergence history of the standard and hierarchical approaches for the fast AD adjusted meshless method. In Figure 11, the corresponding convergence curves using the FVM approach are illustrated. Comparing the figures, one can readily see the superior accuracy of the fast AD adjusted meshless method compared to the FVM approach.

The total computational CPU time using GA and HGA with both the fast AD adjusted meshless method and the FVM approach is shown in Figure 12. The final objective function values are listed on Table II. Based on the superior efficiency and accuracy, the fast AD adjusted meshless method is used in the following test case.

4. A CFD application: optimization of an SCB device on an RAE5243 airfoil

In this section, the hierarchical and standard GAs are applied to a real life optimization problem. For the test case, a lift-constrained optimization problem using a SCB

	GA	HGA Top	HGA Middle	HGA Bottom
Population size	30	10	20 (2 pop)	20 (4 pop)
Crossover rate	0.8	0.8	0.6	0.5
Mutation rate	0.01	0.01	0.02	0.10

Table I. Parameter values for the single-population and HGA

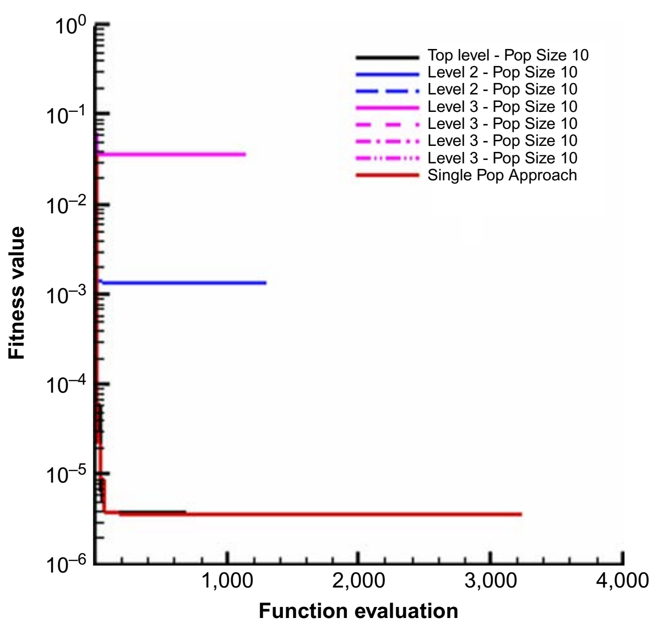

Figure 10. Algorithmic convergence of the hierarchical and standard GAs on the oscillating NACA0012 airfoil case using the fast AD adjusted meshless method

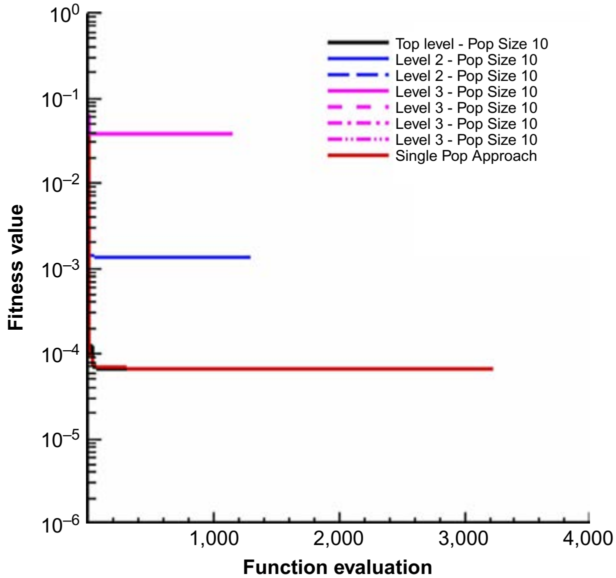

Figure 11.
Algorithmic convergence of the hierarchical and standard GAs on the oscillating NACA0012 airfoil case using the FVM approach

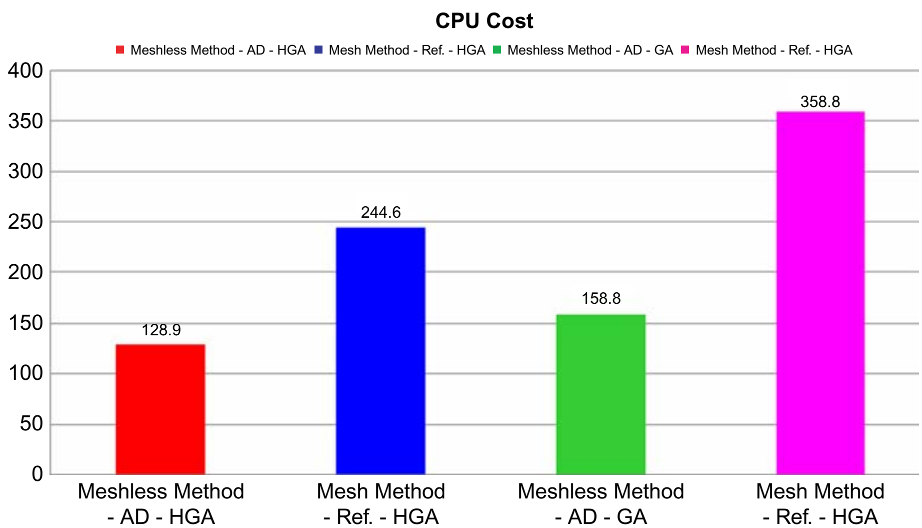

Figure 12.
Comparisons of CPU cost (hours) for the NACA0012 airfoil using standard and HGAs for both the fast AD adjusted meshless method and the FVM approach

installed on an RAE5243 is used. The test case is described in detail in the Finnish Design Test Case Database (test case description is available at the address: http://jucri.jyu.fi/?q=testcase/4).

The objective is to minimize the drag based on the following flow conditions: Mach number is 0.68 and the fixed lift coefficient is 0.82. Figure 13 shows the SCB and the single RAE5243 airfoil baseline. Design variables are defined as bump height, position, length and crest position, as shown in Figure 14. The allowed ranges of the design variables are listed on Table III.

In order to minimize the drag properly, a suitable parameterization of the bump shape is important. In this paper, Bézier splines (Hartmut *et al.*, 2002) are used to define the continuous shape of the SCB.

Both the standard and HGAs operate with the four design parameters and the relaxed iteration based on the angle of attack update in order to satisfy the fixed lift coefficient constraint. Figure 15 shows the Mach number distribution in the flow field with the baseline design.

The standard GA optimization run gives the following final design parameter values for the SCB: Xcrest/C=0.691; Xbumprelative/C = 0.0774; Xbumplength/C = 0.201; ΔYh/C = 0.0296 and the corresponding Mach number distribution in the flow field is shown in Figure 16. It can be seen that the shock is slightly weakened using the SCB.

Table II.
Final objective function values obtained for the standard and HGA using the fast AD adjusted meshless method and the FVM approach

Position reconstruction	Final objective function value
GA (meshless)	3.60695×10^{-006}
HGA (meshless)	3.60454×10^{-006}
GA (mesh)	6.49966×10^{-005}
HGA (mesh)	6.43906×10^{-005}

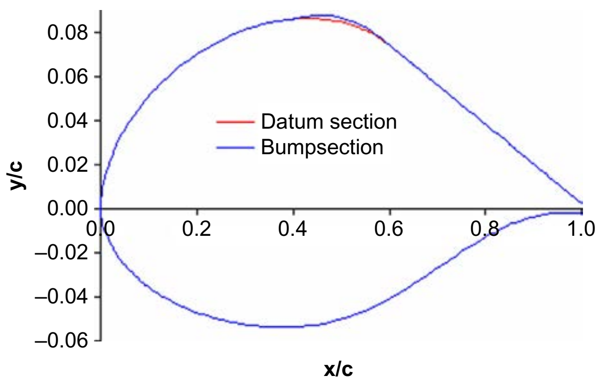

Figure 13.
RAE5243 with SCB

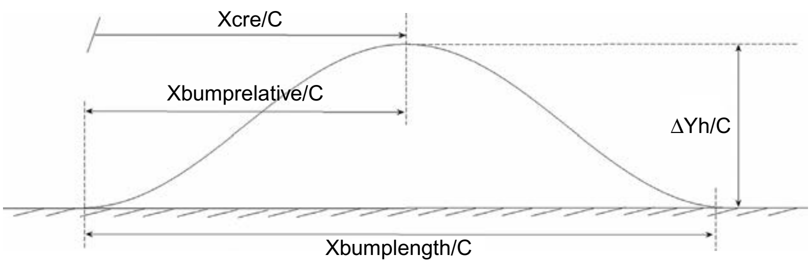

Figure 14.
Bump design parameters

The HGA optimization run gives the following final design parameter values for the SCB: Xcrest/C = 0.705; Xbumprelative/C = 0.0869; Xbumplength/C = 0.254; ΔYh/C = 0.0299 and the corresponding Mach number distribution is shown in Figure 17. It can be seen that the shock is weakened using the SCB, and that the shock is less prominent than in the standard GA case.

The final design parameter values are listed on Table III. The hierarchical approach reduces the drag in this test case by 40.7 percent, compared to only 26 percent of the standard approach (Table IV).

5. Conclusion and future

In this paper, the performances of the standard and HGAs are compared on two optimization problems using an Euler flow analyzer with an innovative and accurate

Table III.
Design parameters for the bump shock reduction test case

Parameter		Min.	Max.
Bump crest position	Xcre/C	0	1
Bump starting point to crest	Xbumprelative/C	0	Xbumplength/C
Bump total length	Xbumplength/C	0	0.4
Bump height	ΔYh/C	0	0.05

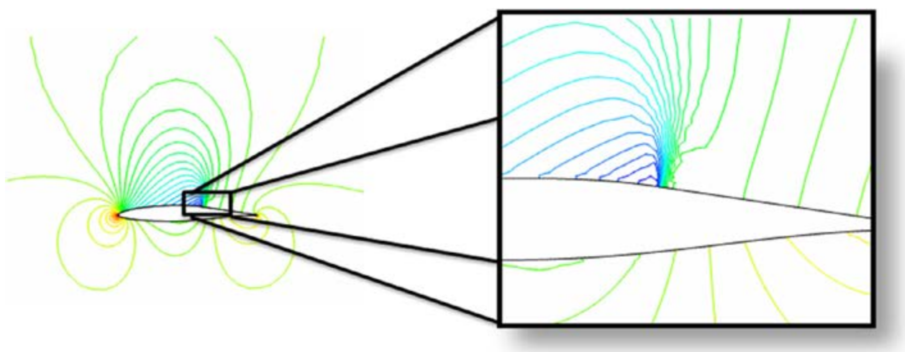

Figure 15.
Mach number distribution in the flow field for the baseline

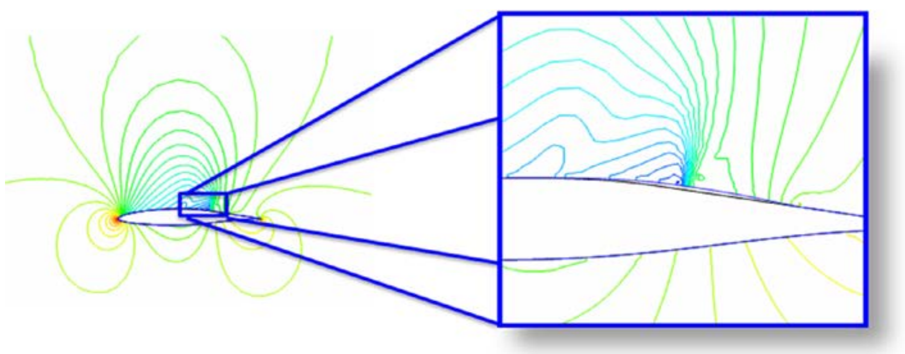

Figure 16.
Mach number distribution in the flow field for the optimized airfoil using the standard GA

fast AD adjusted meshless method, FVM and a hybrid mesh/meshless method. An inverse position reconstruction problem is tested for a single oscillating NACA0012 airfoil using the standard GA and the HGA. Another, more realistic optimization problem consists of drag reduction over a SCB located on a single RAE5243 airfoil operating at transonic flight conditions.

The results demonstrate the superior efficiency and accuracy of the HGA approach over the standard single-population approach, as illustrated in the SCB optimization problem. This can be explained by two reasons. First, by implementing less computational intensive models, computing time can be reduced. This is the underlying idea behind the hierarchical approach. Second, the different levels of explorative behavior can feed the optimization process with new results without losing the exploitative qualities. This is not possible in a single-population GA which is limited to a single model and uniform genetic parameters over the whole population. The results are consistent on both test cases, confirming the validity of the hierarchical approach. Unfortunately computational time restrictions prevented the in-depth study of the algorithmic performances.

Another finding in this paper is the suitability of the fast AD adjusted meshless method for shape optimization. It did not only considerably improve the efficiency, but also produced superior results in the inverse problem and in the drag reduction optimization problem. Furthermore, the results indicate that different flow discretization methods (in this paper, the fast AD adjusted meshless method, hybrid mesh/meshless method, and the FVM) on the different levels of fidelity can work in tandem. This further improves the versatility of the hierarchical approach, since it allows yet another way of introducing variability into the models.

In the near future, our intention is to apply the methods for more complex geometries and more realistic flow models using the mesh/meshless discretization algorithms. Viscous effects such as boundary layers and turbulent Navier-Stokes flows

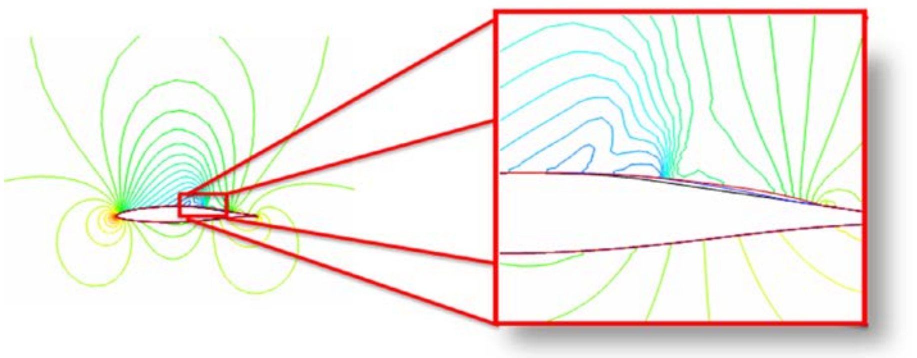

Figure 17. Mach number distribution in the flow field for the optimized airfoil using the HGA

Table IV. SCB design parameters obtained by the standard and HGAs

Bump design	Xcrest/C	Xbumprelative/C	Xbumplength/C	ΔYhv/C	Drag	Drag reduction (%)
Baseline	–	–	–	–	0.02135	–
GA	0.691	0.0774	0.201	0.0296	0.01580	26
HGA	0.705	0.0869	0.254	0.0299	0.01266	40.7

are currently under investigation. In addition, the hierarchical approach studied in this paper will be expanded beyond the traditional GAs into more advanced optimization methods such as the hybrid EAs.

Acknowledgements
The authors would like to thank Hong-Quan Chen for many fruitful discussions on mesh/meshless methods during a visit to the Aerodynamic Department of Nanjing University of Aeronautics and Astronautics (NUAA), China; Mourad Sefrioui whose HGAs evolutionary approach inspire this study applied to mesh/meshless Euler solvers and also Ning Qin for active interactions about the physical and numerical aspects of the SCB device optimization problem test case problem that he defined in the Finnish Database Workshop held in Jyväskylä in 2010. The Finnish Funding Agency for Technology and Innovation (TEKES) is acknowledged for funding the DESIGN project and partially supporting this research and also we are grateful to Pekka Neittaanmäki, Dean of Faculty of Information Technology, for his guidance and help with Finnish Doctoral Programme in Computational Sciences (FICS), Jyväskylä Doctoral Program in Computing and Mathematical Sciences (COMAS) and the Department of Mathematical Information Technology, Jyväskylä, Finland.

References

Batina, J.T. (1992), "A gridless Euler/Navier-stokes solution algorithm for complex two-dimensional applications", NASA-TM-107631, June.

Belytschko, T., Lu, Y.Y. and Gu, L. (1994), "Element-free Galerkin methods", *International Journal for Numerical Methods in Engineering*, Vol. 37, pp. 229-256.

Berger, M.J. and LeVeque, R.J. (1989), "An adaptive Cartesian mesh algorithm for the Euler equations in arbitrary geometries", AIAA Paper 1989-1930.

Blazek, J. (2001), *Computational Fluid Dynamics: Principles and Applications*, Elsevier Science, Amsterdam.

Chen, H.Q. (2003), "Implicit gridless method for Euler equations", *Chinese Journal of Computational Physics*, Vol. 20 No. 1, pp. 9-13.

Chen, H.Q. and Shu, C. (2005), "An efficient implicit mesh-free method to solve two-dimensional compressible Euler equations", *International Journal of Modern Physics C*, Vol. 16 No. 3, pp. 439-454.

Deb, K. (2002), *Multi-objective Optimization Using Evolutionary Algorithms*, Wiley, Chichester.

Eshelman, L.J. and Schaffer, J.D. (1993), "Real-coded genetic algorithms and interval-schemata", in Whitley, L.D. (Ed.), *Foundations of Genetic Algorithms 2*, Morgan Kaufmann, San Mateo, CA, pp. 187-202.

Farhat, C., Degand, C., Koobus, B. and Lesoinne, M. (1998), "An improved method of spring analogy for dynamic unstructured fluid meshes", AIAA Paper 98-2070.

Ghosh, A.K. and Deshpande, S.M. (1995), "Least squares kinetic upwind method for inviscid compressible ?ows", AIAA paper 1995-1735, paper presented at AIAA 12th Computational Fluid Dynamics Conference, San Diego, CA, June.

Godunov, S.K. (1969), "A difference scheme for numerical solution of discontinuous solution of hydrodynamic equations", *Math. Sbornik*, Vol. 47, pp. 271-306 (translated US Joint Publ. Res. Service, JPRS 7226).

Goldberg, D.E. (1989), *Genetic Algorithms in Search, Optimization, and Machine Learning*, Addison-Wesley, Boston, MA.

Gorges-Schleuter, M. (1992), "Comparison of local mating strategies in massively parallel genetic algorithms", *Proceedings of the Second Conference on Parallel Problem Solving from Nature*, pp. 553-562.

Hartmut, P., Wolfgang, B. and Marco, P. (2002), *Bezier and B-spline Techniques*, Springer, Berlin.

Jameson, A. and Mavriplis, D. (1986), "Finite volume solution of the two-dimensional Euler equations on a regular triangular mesh", *AIAA Journal*, Vol. 24, pp. 611-618.

Jameson, A., Schmidt, W. and Turkel, E. (1981), "Numerical solution of the Euler equations by finite volume methods using Runge-Kutta time-stepping schemes", paper presented at AIAA 14th Fluid and Plasma Dynamics Conference, 23-25 June.

Lee, D.S., Periaux, J., Gonzalez, L.F., Srinivas, K. and Onate, E. (2010), "Active flow control bump design using hybrid Nash-game coupled to evolutionary algorithms", in Pereira, J.C.F. and Sequeira, A. (Eds), *Proceedings of V European Conference on Computational Fluid Dynamics ECCOMAS CFD 2010, Lisbon, Portugal, 14-17 June*, pp. 1-14.

Liu, X.Q., Qin, N. and Xia, H. (2006), "Fast dynamic grid deformation based on Delaunay graph mapping", *Journal of Computational Physics*, Vol. 211 No. 2, pp. 405-423.

Luo, H. and Baumy, J.D. (2005), "A hybrid Cartesian grid and gridless method for compressible flow", paper presented at 43rd AIAA Aerospace Sciences Meeting and Exhibit, Reno, Nevada, 10-13 January.

Ma, Z.H., Chen, H.Q. and Wu, X.J. (2006), "A gridless-finite volume hybrid algorithm for Euler equations", *Chinese Journal of Aeronautics*, Vol. 19 No. 4, pp. 286-294.

Michalewicz, Z. (1992), *Genetic Algorithm+Data Structures=Evolution Programs*, Springer, New York, NY.

Miettinen, K.M. (1999), *Nonlinear Multiobjective Optimization*, Kluwer Academic, Boston, MA.

Morinishi, K. (2001), "An implicit gridless type solver for the Navier-Stokes equations", *Computational Fluid Dynamics*, pp. 551-560.

Osher, S.J. (1983), "Shock modelling in aeronautics", in Baines, M. and Morton, K.W. (Eds), *Numerical Methods in Fluid Dynamics*, Academic Press, Waltham, MA, pp. 179-217.

Pettey, C.B., Leuze, M.R. and Grefenstette, J.J. (1987), "A parallel genetic algorithm", *Proceedings of the Second International Conference on Genetic Algorithms*.

Pulliam, T.H. (1986), "Artificial dissipation models for the Euler equations", *AIAA Paper*, Vol. 24 No. 12.

Pulliam, T.H. and Steger, J.L. (1985), "Recent improvements in efficiency, accuracy, and convergence for implicit approximate factorization algorithms", AIAA 85-0360.

Qin, N., Wong, W.S. and Le Moigne, A. (2008), "Three-dimensional contour bumps for transonic wing drag reduction", *Proceedings of the Institution of Mechanical Engineers G, Journal of Aerospace Engineering*, Vol. 222 No. 5, pp. 619-629.

Qin, N., Zhu, Y. and Shaw, S.T. (2004), "Numerical study of active shock control for transonic aerodynamic", *International Journal of Numerical Methods for Heat & Fluid Flow*, Vol. 14 No. 4, pp. 444-466.

Roe, P. (1981), "Approximate Riemann solvers, parameter vectors, and difference schemes", *Journal of Computational Physics*, Vol. 43, pp. 357-372.

Schlierkamp-Voosen, D. and Muhlenbein, H. (1994), "Strategy adaptation by competing subpopulations", *Parallel Problem Solving from Nature – PPSN III International Conference on Evolutionary Computation*, pp. 199-208.

Sefrioui, M. and Périaux, J. (2000), "A hierarchical genetic algorithm using multiple models for optimization", in Schoenauer, M., Deb, K., Rudolph, G., Yao, X., Lutton, E., Merelo, J.J. and Schwefel, H.-P. (Eds), *Parallel Problem Solving from Nature, PPSN VI*, Springer, Berlin, pp. 879-888.

Van Leer, B. (1979), "Towards the ultimate conservative difference scheme. V a second order sequel to Gudonov's method", *Journal of Computational Physics*, Vol. 32, pp. 101-136.

Wang, H., Chen, H.Q. and Periaux, J. (2010), "A study of gridless method with dynamic clouds of points for solving unsteady CFD problems in aerodynamics", *International Journal for Numerical Methods in Fluids*, Vol. 64 No. 1, pp. 98-118.

About the authors

Hong Wang was born in China, on March 4, 1983. She received the B.E. degree in Aircraft and Aerospace Engineering and the M.E. degree in Fluid Dynamics in Nanjing University of Aeronautics and Astronautics, Nanjing, China, in 2006 and 2009, respectively. She received a PhD degree in Scientific Computing from the University of Jyväskylä, Jyväskylä, Finland, in 2012. Her areas of expertise include evolutionary algorithms, Nash game strategy, hybrid games, computational fluid dynamics, meshless methods, hybrid mesh/meshless methods, mesh/meshless adaption, multi-disciplinary/multi-physics design optimization (MDO), and parallel computing. Hong Wang is the corresponding author and can be contacted at: hong.m.wang@jyu.fi

Jyri Leskinen was born in Finland, on October 25, 1976. He received an MSc degree and a PhD degree from the University of Jyväskylä, Jyväskylä, Finland, in 2007 and 2012, respectively. His areas of expertise include shape design optimization using evolutionary algorithms including hybridized methods, parallel computing using game strategies and scientific computing on graphic processing units (GPUs).

Dong-Seop Lee was born in Korea, on January 26, 1976. He received the B.E. degree in Aerospace Mechanical Mechatronic Engineering and a PhD degree from the School of Aerospace Mechanical Mechatronic Engineering (AMME)-Honor, University of Sydney, Sydney, Australia, in 2004 and 2008, respectively. He is currently a Researcher with the International Center for Numerical Methods in Engineering (CIMNE)/UPC, Barcelona, Spain for European Projects. His areas of expertise include computational fluid dynamics, multiobjective and multidisciplinary design optimization in aerospace engineering, evolutionary algorithms, game strategies, and robust/uncertainty design. He has published two book chapters, and five journal papers. His current research interests are efficient optimization methods, unmanned aerial systems (UAS), and mission trajectory planning systems (MTPS).

Jacques Périaux was born in France, on April 15, 1942. He received a PhD degree from the University of Paris, Paris, France, in 1979. He is currently a United Nations Educational, Scientific and Cultural Organization Chair with the International Center for Numerical Methods in Engineering (CIMNE)/UPC and also the Finland Distinguished Professor Programme at University Jyväskylä, Jyväskylä, Finland. His areas of expertise include numerical solution of nonlinear partial differential equations in computational fluid dynamics and electromagnetic, aerodynamic design of manned/unmanned aircraft vehicles, multidisciplinary design optimization, evolutionary algorithms, and game theory.